Soil Dynamics and Earthquake Engineering 143 (2021) 106627

Contents lists available at ScienceDirect

Soil Dynamics and Earthquake Engineering

journal homepage: http://www.elsevier.com/locate/soildyn

Review

Seismic vulnerability assessment of buried pipelines: A 3D parametric study

Claudia Germoso [a,*], Omar Gonzalez [b], Francisco Chinesta [c]

[a] Instituto Tecnológico de Santo Domingo (INTEC). Av. Los Próceres, Jardines del Norte, 10602, Santo Domingo, Dominican Republic
[b] Universidad INCE, Av. Gustavo Mejía Ricart No. 211, Santo Domingo, Dominican Republic
[c] ESI GROUP Chair @ PIMM, Arts et Métiers Institute of Technology, 151 Boulevard de l'Hopital, F-75013, Paris, France

ARTICLE INFO

Keywords:
Soil-pipeline interaction seismic vulnerability nonlinear soil behavior proper generalized decomposition (PGD) in-plane-out-of-plane separated representation

ABSTRACT

Pipeline structural analysis is a well-developed topic in engineering and research practice. Since water, oil or gas pipeline systems are a key part of modern development, therefore, it is important to ensure an appropriate behavior under seismic action. In this paper, the seismic response of buried pipelines is numerically simulated using a three-dimensional (3D) parametric model of soil-pipeline interaction. The role of several parameters on both soil and pipeline are incorporated into a 2D-1D space separated representation based on the Proper Generalized Decomposition (PGD) framework, which allows addressing 3D parametric problems while reducing the computational complexity of 1D and 2D characteristic problems. These results can be used for design, safety evaluation and protection of buried pipelines crossing seismic area and can be calculated in real time from the parametric solution of the associated problem within the PGD framework.

1. Introduction

Strong ground shaking is the most damaging earthquake hazard. It is a result of rapid ground acceleration due to the seismic waves passing, and vary from quite gentle in small earthquakes to incredibly violent in large earthquakes. Seismic response analysis has been extensively studied in buildings, roads, and other structures above ground. However, the seismic behavior is entirely different in underground structures as pipeline systems, therefore, structural or geotechnical failures are causes of uncertainty and extensive investigations have been carried out to reveal this problem.

Pipeline, often referred as lifeline systems, carry essential services to the functioning and support of day-to-day life, such as energy systems, water treatment, transportation and information systems, which requires continues services even after damaging earthquakes. City underground pipeline systems around the world have been suffered severely damages in recent earthquakes, such as Loma Prieta (USA, 1989) [15], Northridge of California (USA, 1994) [29], Kobe (Japan, 1995) [28], Kocaeli (Turkey, 1999) [1] and Ji-Ji earthquake (Taiwan, 1999) [8] are the most famous examples of lifeline failures, that mainly affected the water and gas systems where not only normal usage functions were damaged, but also derivative calamities were brought.

These systems are greatly affected by three major causes, including ground conditions, seismic intensity and lifeline features [2]. The soil-pipeline interaction problem is generally analyzed as two dimensional (2D) numerical calculation, although the system is clearly three dimensional (3D). Two dimensional assumption could be very different from the observed values at the site, therefore, it is necessary to develop 3D numerical calculation, which is closer to the real problem and more suitable for engineering design. A perfect characterization of the seismic response of buried pipeline, must consider a 3D dynamic analysis of the soil-pipeline interaction under multipoint earthquake excitation and investigate the effect of important parameters related to the soil, pipeline and input motion.

Three dimensional (3D) parametric solutions seem mandatory in many cases, however, this model severely increase modeling complexity and computational cost in terms of the enormous number of degrees of freedom. The separated representation within the Proper Generalized Decomposition (PGD) framework seems to be a valuable route for alleviating such problem [9–11,24].

In this research, the role of several parameters on both the pipeline and soil are extensively studied based on the PGD framework. A possibility for circumventing the issues related to the large numbers of degrees of freedom of fully 3D mesh-based discretization, consists in reducing the model complexity making use of an in-plane-out-of-plane separated representation, that allows considering the solution of high-resolution 3D models at the cost of usual 2D solutions. This decomposition for solving 3D problems can be perfertly applied to shell, plate or

* Corresponding author.
E-mail addresses: claudia.germoso@intec.edu.do (C. Germoso), mgonzalez1@ince.edu.do (O. Gonzalez), Francisco.Chinesta@ensam.eu (F. Chinesta).

https://doi.org/10.1016/j.soildyn.2021.106627
Received 9 October 2020; Received in revised form 22 January 2021; Accepted 23 January 2021
Available online 11 February 2021

extruded domains [4,6,7,19].

The mechanical behavior of the buried pipeline will be described considering the nonlinearity aspects of soil, in which an efficient nonlinear solver is proposed. These results are intended to guide and define the buried pipe networks towards more optimal design for the pipeline performance and its mechanical reliability.

2. Elasto-dynamic problem. In-plane-out-of-plane separated representation

In what follows, the construction of the separated representation within the PGD framework is described. We consider the in-plane-out-of-plane decomposition which allows to address 3D problems while reducing the computational complexity of 1D and 2D characteristic problems.

According to the PGD framework, the displacement field for a fully three dimensional solution $\mathbf{u}(x,y,z,t)$ can be written using a separated representation as,

$$\mathbf{u}(x,y,z,t)=\begin{pmatrix} u(x,y,z,t)\\ v(x,y,z,t)\\ w(x,y,z,t)\end{pmatrix}\approx\sum_{i=1}^{M}\begin{pmatrix} \mathscr{X}^i_{\mathrm{u}}(x)\cdot\mathscr{Y}^i_{\mathrm{u}}(y)\cdot\mathscr{Z}^i_{\mathrm{u}}(z)\cdot\mathscr{T}^i(t)\\ \mathscr{X}^i_{\mathrm{v}}(x)\cdot\mathscr{Y}^i_{\mathrm{v}}(y)\cdot\mathscr{Z}^i_{\mathrm{v}}(z)\cdot\mathscr{T}^i(t)\\ \mathscr{X}^i_{\mathrm{w}}(x)\cdot\mathscr{Y}^i_{\mathrm{w}}(y)\cdot\mathscr{Z}^i_{\mathrm{w}}(z)\cdot\mathscr{T}^i(t)\end{pmatrix}, \tag{1}$$

where $(x,y,z,t)\in\Im$, with $\Im=\Omega_x\times\Omega_y\times\Omega_z\times\Omega_t$. The above equation can be expressed in a more compact form

$$\mathbf{u}(x,y,z,t)\approx\sum_{i=1}^{M}\mathbf{X}^i(x)\circ\mathbf{Y}^i(y)\circ\mathbf{Z}^i(z)\circ\mathbf{T}^i(t), \tag{2}$$

where "$\circ$" stands for Hadamard (component wise) product.

Solving 3D models in degenerated domains, as shell/plate geometry, in which one dimension is very small in comparison with the others, are abundantly solved in many engineering applications. In such cases, the 3D model can be separated using an in-plane-out-of-plane separated representation given by

$$\mathbf{u}(x,y,z,t)\approx\sum_{i=1}^{M}\mathbf{X}^i(x,y)\circ\mathbf{Z}^i(z)\circ\mathbf{T}^i(t), \tag{3}$$

with $\Im=\Omega_{xy}\times\Omega_z\times\Omega_t$, where $(x,y)\in\Omega_{xy}\subset\Re^2$ and $z\in\Omega_z=(0,L)$. Vectors $\mathbf{X}^i$ are the functions in-plane coordinates (x,y), $\mathbf{Z}^i$ are the functions involving the z-coordinate (model length) and $\mathbf{T}^i$ are functions related to time (t). This formulation seems again the most appealing route for addressing 3D discretizations while keeping the computational complexity of 2D problems. Is important to know that the above functions are not known a priori but are calculated by introducing the separated representation of the solution in the weak formulation of the problem resulting in a nonlinear problem. Which requires an iteration process in each enrichment step.

Let's consider a dynamic elasticity problem in $\Im$, the displacement field $\mathbf{u}(x,y,z,t)$ is governed by the following equation

$$\rho\ddot{\mathbf{u}}=\nabla\cdot\sigma. \tag{4}$$

By moving to the Fourier space, the problem involves the displacement amplitude, that for the sake of notational simplicity continues being noted as $\mathbf{u}$, with components (u,v,w), all them depending on the space (x,y,z) and the frequency (ω).

The weak formulation writes as follows

$$-\int_{\Omega}\mathbf{u}^*\rho\omega^2\mathbf{u}\,d\Omega=-\int_{\Omega}\varepsilon^*\mathbf{D}\,\varepsilon\,d\Omega+\int_{\Omega}\mathbf{u}^*\mathbf{F}\,d\Omega, \tag{5}$$

with $\Omega=\Omega_{xy}\times\Omega_z$, where ρ is the density, ω is the frequency, $\mathbf{F}$ is the volumetric body forces in the frequency space and $\mathbf{D}$ is the linear elastic isotropic material given by the generalized 6×6 Hooke tensor,

$$\mathbf{D}=\begin{bmatrix}\lambda+2\mu & \lambda & \lambda & 0 & 0 & 0\\ \lambda & \lambda+2\mu & \lambda & 0 & 0 & 0\\ \lambda & \lambda & \lambda+2\mu & 0 & 0 & 0\\ 0 & 0 & 0 & \mu & 0 & 0\\ 0 & 0 & 0 & 0 & \mu & 0\\ 0 & 0 & 0 & 0 & 0 & \mu\end{bmatrix}, \tag{6}$$

where

$$\lambda=\frac{\nu E}{(1+\nu)(1-2\nu)} \tag{7}$$

and

$$\mu=\frac{E}{2(1+\nu)}, \tag{8}$$

are the Lame's constants, E and ν are the Young modulus and the Poisson coefficient, respectively. Now, using the following definitions for the strain vector

$$\varepsilon=\begin{bmatrix}\varepsilon_x\\ \varepsilon_y\\ \varepsilon_z\\ \gamma_{xy}\\ \gamma_{yz}\\ \gamma_{xz}\end{bmatrix}=\begin{bmatrix}\dfrac{\partial u}{\partial x}\\ \dfrac{\partial v}{\partial y}\\ \dfrac{\partial w}{\partial z}\\ \dfrac{\partial u}{\partial y}+\dfrac{\partial v}{\partial x}\\ \dfrac{\partial v}{\partial z}+\dfrac{\partial w}{\partial y}\\ \dfrac{\partial u}{\partial z}+\dfrac{\partial w}{\partial x}\end{bmatrix}, \tag{9}$$

the separated representation of (5), assuming the frequency as an extra coordinate, can be expressed as

$$\mathbf{u}(x,y,z,\omega)=\begin{pmatrix} u(x,y,z,\omega)\\ v(x,y,z,\omega)\\ w(x,y,z,\omega)\end{pmatrix}\approx\sum_{k=1}^{N}\mathbf{X}^k(x,y)\circ\mathbf{Z}^k(z)\circ\mathbf{W}^k(\omega), \tag{10}$$

with vectors $\mathbf{W}^k$ the functions related with the frequency (ω).

Supposing that $\mathbf{u}^{n-1}$ to be known, the computation of the next functional product $\mathbf{X}^n(x,y)$, $\mathbf{Z}^n(z)$ and $\mathbf{W}^n(\omega)$ is given by

$$\mathbf{u}^n(x,y,z,\omega)=\mathbf{u}^{n-1}(x,y,z,\omega)+\mathbf{X}^n(x,y)\circ\mathbf{Z}^n(z)\circ\mathbf{W}^n(\omega), \tag{11}$$

and the test function $\mathbf{u}^*$ reads

$$\mathbf{u}^*(x,y,z,\omega)=\begin{pmatrix} \mathscr{X}^*_u\cdot\mathscr{Z}^n_u\cdot\mathscr{W}^n_u+\mathscr{X}^n_u\cdot\mathscr{Z}^*_u\cdot\mathscr{W}^n_u+\mathscr{X}^n_u\cdot\mathscr{Z}_u\cdot\mathscr{W}^*_u\\ \mathscr{X}^*_v\cdot\mathscr{Z}^n_v\cdot\mathscr{W}^n_v+\mathscr{X}^n_v\cdot\mathscr{Z}^*_v\cdot\mathscr{W}^n_v+\mathscr{X}^n_v\cdot\mathscr{Z}_v\cdot\mathscr{W}^*_v\\ \mathscr{X}^*_w\cdot\mathscr{Z}^n_w\cdot\mathscr{W}^n_w+\mathscr{X}^n_w\cdot\mathscr{Z}^*_w\cdot\mathscr{W}^n_w+\mathscr{X}^n_w\cdot\mathscr{Z}_w\cdot\mathscr{W}^*_w\end{pmatrix}, \tag{12}$$

or

$$\mathbf{u}^*(x,y,z,\omega) = \mathbf{X}^* \circ \mathbf{Z}^n \circ \mathbf{W}^n + \mathbf{X}^n \circ \mathbf{Z}^* \circ \mathbf{W}^n + \mathbf{X}^n \circ \mathbf{Z}^n \circ \mathbf{W}^*. \tag{13}$$

Finally, considering Eqs. (6), (9) and (10), the resulting weak form (5) reads now

$$-\int_\Gamma \left[u^*\rho\omega^2 u + v^*\rho\omega^2 v + w^*\rho\omega^2 w \right] d\Gamma = -\int_\Gamma \left[\varepsilon_x^*\theta\varepsilon_x + \varepsilon_y^*\lambda\varepsilon_x + \varepsilon_z^*\lambda\varepsilon_x + \varepsilon_x^*\lambda\varepsilon_y + \varepsilon_y^*\theta\varepsilon_y + \varepsilon_z^*\lambda\varepsilon_y + \right.$$

$$\left. \varepsilon_x^*\lambda\varepsilon_z + \varepsilon_y^*\lambda\varepsilon_z + \varepsilon_z^*\theta\varepsilon_z + \gamma_{xy}^*\mu\gamma_{xy} + \gamma_{yz}^*\mu\gamma_{yz} + \gamma_{xz}^*\mu\gamma_{xz} \right] d\Gamma, \tag{14}$$

where $\theta = \lambda + 2\mu$. Now, with (9) in its separated form and Eqs. (11) and (13) into (14) results a nonlinear problem.

Simplest linearization strategy based on alternated directions of fixed-point iterations is applied, which proceed by assuming sequentially that $\mathbf{Z}^{n,p-1}(z)$ and $\mathbf{W}^{n,p-1}(\omega)$ are known of the previous iteration, and proceed to compute $\mathbf{X}^{n,p}(x,y)$. With $\mathbf{X}^{n,p}(x,y)$ already known and $\mathbf{W}^{n,p-1}(\omega)$, is computed $\mathbf{Z}^{n,p}(z)$. Finally, with $\mathbf{X}^{n,p}(x,y)$ as well as $\mathbf{Z}^{n,p}(z)$ known, $\mathbf{W}^{n,p}(z)$ can be obtained. The process is repeated in a suitable fixed-point iteration scheme, until reaching a state of convergence, where the results will be the new products $\mathbf{X}^n(x,y)$, $\mathbf{Z}^n(z)$ and $\mathbf{W}^n(\omega)$. The enrichment stop when the model residual become small enough.

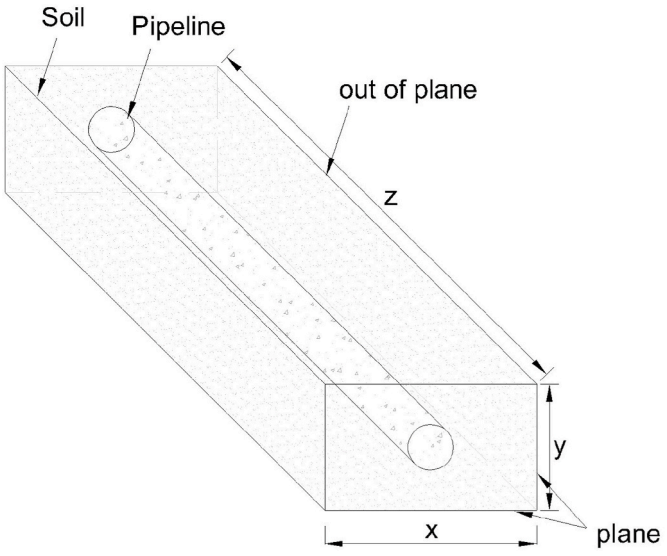

Fig. 1. Soil-pipeline model.

First, we assume $\mathbf{Z}^n(z)$ and $\mathbf{W}^n(\omega)$ to be known from the previous iteration, in this case the test function is $\mathbf{u}^* = \mathbf{X}^*(x,y) \circ \mathbf{Z}^n(z) \circ \mathbf{W}^n(\omega)$. Introducing the separated representation of the solution at iteration n (Eq. (11)), the test function into (14) and then integrating in Ω_{xy}, the resulting 2D equation can be interpreted as the weak formulation in which the unknown function $\mathbf{X}^n(x,y)$ is obtained using any suitable discretization techniques.

Second, with the new values of $\mathbf{X}^n(x,y)$ and $\mathbf{W}^n(\omega)$ previously assumed, the test function is chosen equal to $\mathbf{u}^* = \mathbf{X}^n(x,y) \circ \mathbf{Z}^*(z) \circ \mathbf{W}^n(\omega)$. By introducing (11) and the test function into the weak formulation (14) and integrating in Ω_z, we obtain the resulting 1D weighted residual form which can be solved by using any discretization techniques to obtain the unknown function $\mathbf{Z}^n(z)$.

Finally, with $\mathbf{X}^n(x,y)$ and $\mathbf{Z}^n(z)$ already updated, the test function now reads $\mathbf{u}^* = \mathbf{X}^n(x,y) \circ \mathbf{Z}^n(z) \circ \mathbf{W}^*(\omega)$. With (11) and the test function into (14) and integrating over Ω_ω allows computing function $\mathbf{W}^n(\omega)$ (see Refs. [10–12] for more details).

3. Nonlinear seismic ground response analysis

To evaluate the dynamic response of a soil and soil-pipe systems, soil properties such as shear modulus G and damping ratio ζ need to be known. These properties present nonlinear behavior regarding the strain level, even without reflect the possible development of permanent deformation. Soil stiffness is normally characterized by the small-strain shear modulus G_{max} which degrades as the level of shear strain increases, and the dissipative soil behavior is characterized by the damping ratio ζ that grows with increasing the amplitude of shear strain [30]. According to these dependencies, the problem becomes highly nonlinear and an iteration method is required to reach a compatibility between the properties used in the analysis and the computed strain.

In the case of simple harmonic excitation, damping is usually expressed by using a complex and frequency-dependent stiffness. The soil model can be represented by the constitutive relationship between the stress and strain from a Kelvin-Voigt (KV) three-dimensional model, as an extension of the well-known KV one-dimensional model [23]. Thus, the shear stress can be expressed as

$$\sigma = \mathbf{D}\varepsilon + \mathbf{D}\varepsilon\frac{d\varepsilon}{dt}, \tag{15}$$

or in the frequency domain

$$\sigma = (\mathbf{D} + i\omega\mathbf{D}')\varepsilon, \tag{16}$$

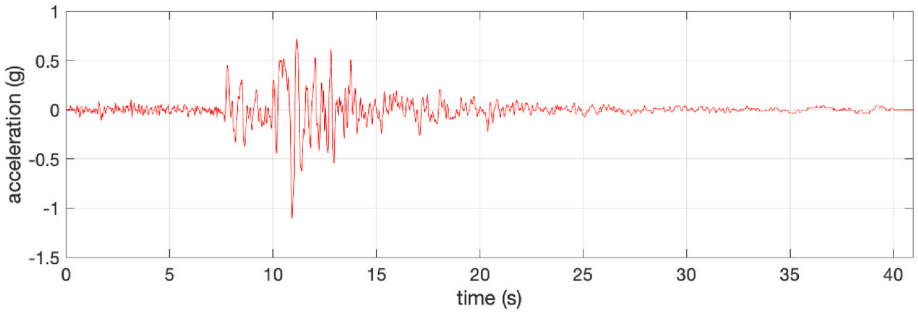

Fig. 2. Recorded horizontal ground motions at a site.

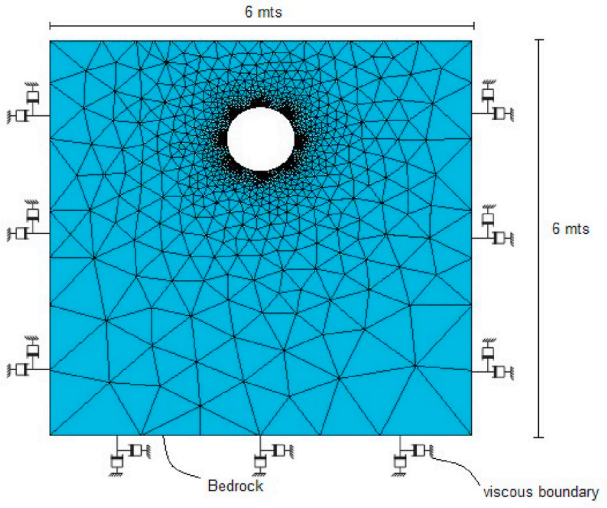

Fig. 3. Pipeline-soil model mesh and boundary condition.

where tensor **D** is defined as dependence on the Elastic modulus E and the Poisson coefficient ν (Eq. (6)), and $\mathbf{D}'$ involves the viscosity modulus $\eta = \frac{2E\zeta}{\omega}$. Now, taking into account the damping coefficient of soil, the Lame's constants given in Eq. (7) (8) can be rewritten for soil as

$$\overline{\lambda}_s = (E + i2E\zeta)\frac{\nu_s}{(1+\nu_s)(1-2\nu_s)} = (1+i2\zeta)\lambda_s, \tag{17}$$

and

$$\overline{\mu}_s = (E + i2E\zeta)\frac{1}{2(1+\nu_s)} = (1+i2\zeta)\mu_s, \tag{18}$$

where $\overline{\lambda}_s$ and $\overline{\mu}_s$ are the complex Lame's constants of soil [3].

Lysmer and Kuhlemeyer [20] transmitting boundary condition is implemented with the aim to avoiding reflected waves from boundaries of finite domains. As a result, waves arriving at the boundary can be absorved by dashpots positioned normal and tangential (x-normal- and (y, z)-tangential- in the lateral surfaces, and z-normal- and (x, y)-tangential- in the frontal and posterior surfaces) to the boundary. These conditions are considered to absorb the plane waves, taking into account the three directions independently, by assigning equivalent dashpots on the boundary (see Fig. 3). These can be defined as stresses in the lateral surfaces [27],

$$\begin{aligned} \sigma_x &= c_p\rho i\omega u \\ \tau_{xy} &= c_s\rho i\omega v \\ \tau_{xz} &= c_s\rho i\omega w \end{aligned} \tag{19}$$

and in the frontal and posterior surfaces

$$\begin{aligned} \sigma_z &= c_p\rho i\omega w \\ \tau_{zx} &= c_s\rho i\omega u \\ \tau_{zy} &= c_s\rho i\omega v \end{aligned} \tag{20}$$

where ρ is the density, c_s the S-wave (shear wave) and c_p the P-wave (compressional wave) speeds.

Meanwhile, the seismic loading is applied at soil-bedrock from the rock outcropping motion time histories $\ddot{y}$ (assumed measurable), and a linear dashpot is localized at the base of the soil column acting in different directions of motion, as an absorbing boundary condition (see Refs. [13,16,25] for more details). Thus, the half-space (bedrock) is replaced with an equivalent shear stress time history

$$\begin{aligned} \tau_{yx} &= c_s^*\rho_b\dot{y}_x - c_s^*\rho_b i\omega u \\ \sigma_y &= c_p^*\rho_b\dot{y}_y - c_p^*\rho_b i\omega v \\ \tau_{yz} &= c_s^*\rho_b\dot{y}_z - c_s^*\rho_b i\omega w \end{aligned} \tag{21}$$

where c_s^*, c_p^* and ρ_b are S-wave velocity, P-wave velocity and the density at bedrock, respectively. The first terms in the right hand member of the above equation correspond to the forces, $\mathbf{F}(t) = (F_x, F_y, F_z)$ acting in the different directions (x, y, z) and the second are dashpots to mimic the infinite half space at the bottom of the soil column.

Table 1
Pipeline properties for different materials.

Material	Elastic modulus MPa	Density (kg/m^3)
Polyethylene (PE)	200–400	920–960
PVC	3000	1370–1420
Polypropylene (PP)	1200–1800	900
Concrete	2e4 - 4e4	2300
Steel	2.1e5	7800

3.1. Equivalent linear approximation

The equivalent linear approximation method [22] is implemented to address the nonlinear soil behavior. It has been used in several computer programs for site response analysis, as EERA [5], and SHAKE software [26] for one dimensional analysis and FLUSH [21], QUAD4 [14] and TLUSH [17] for two and three dimensional analysis. According to this approximation, the nonlinear soil response can be approximated by a linear analysis for which the shear modulus G and the damping ratio ζ are compatible with the effective shear strain amplitude [18].

As described in (9), the three dimensional strain tensor is given by

$$\varepsilon = [\,\varepsilon_x \quad \varepsilon_y \quad \varepsilon_z \quad \gamma_{xy} \quad \gamma_{yz} \quad \gamma_{xz}\,]^T. \tag{22}$$

Soil behavior depends on all terms of this expression, directional and time variation. However, the constitutive laws of soil does not permit a completed characterization of the material. Thus, the equivalent linear method assume an effective strain given by the peak maximum shear strain,

$$\gamma_{eff} = \frac{2}{3}\gamma_{max}, \tag{23}$$

(~ 66 % of the peak strain). The above equation can be computed by two different procedures. First, obtaining the maximum strains, which requires to come back to the time domain to evaluate the maximum shear strain and from it the peak maximum. Second, approximate the maximum shear strain making use of the Root Mean Square (RMS) value in frequency domain as follows

$$\gamma_{max} \approx C\cdot\mathrm{RMS}\left(\gamma_{max}^*\right), \tag{24}$$

with

$$C = \frac{\max|\ddot{y}(t)|}{\mathrm{RMS}(\ddot{y})}, \tag{25}$$

where $\ddot{y}$ is input motion known as the rock outcropping motion (assumed measurable) and γ_{max}^* is the maximum shear strain which can be obtained from the principal strains of (22) in terms of the strain complex amplitudes for each frequency. The RMS value of γ_{max}^* and $\ddot{y}$ can be evaluated using the Parseval' identity

$$\mathrm{RMS}^2 = \frac{1}{2}\sum_{s=0}^{N/2}\left|F_s\right|^2, \tag{26}$$

where F_s, $s = 0, 1, \ldots, N/2$, are the complex Fourier amplitudes. Finally, the effective strain can be rewritten as

$$\gamma_{eff} = \frac{2}{3}\frac{\max|\ddot{y}(t)|}{\mathrm{RMS}(\ddot{y})}\mathrm{RMS}\left(\gamma_{max}^*\right). \tag{27}$$

This is reasonable since strains are essentially proportional to the input acceleration. The first procedure is the most effective, however, it

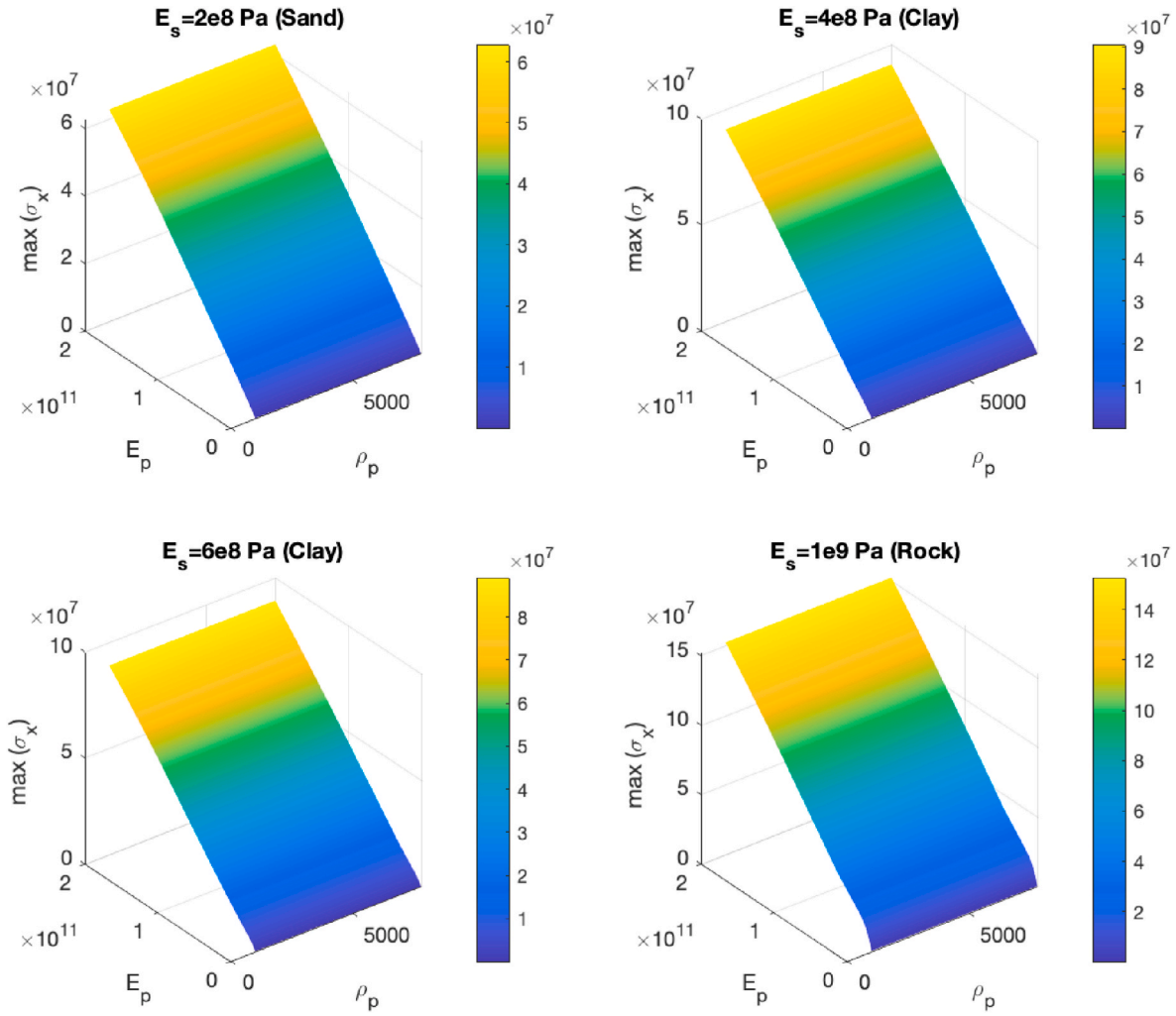

Fig. 4. Maximum stress (σ_x) versus pipeline elastic modulus and density considering different soil models.

is very expensive, since it requires numerous Fast Fourier Transforms and considerable computer time and storage, while the second procedure is inexpensive and the difference between the two approaches is less than 15%.

4. PGD-based parametric solutions

This section describes the parametric solution within the PGD framework. The in-plane-out-of-plane decomposition detailed in section 2 will be applied to the soil-pipeline model (Fig. 1), allowing consider the solution of high resolution 3D models at the cost of usual 2D solutions. The model is assumed composed of $\mathscr{T}$ materials $\delta_i, i = 1,\ldots,\mathscr{T}$, the ones related to the soil layers and the one related to the pipeline. Each material is identified from its characteristic function $\chi_i(\alpha), i = 1,\cdots,\mathscr{T}$, defined as

$$\chi_i(\alpha) = \begin{cases} 1 & \text{if} \quad \alpha \in \delta_i \\ 0 & \text{if} \quad \alpha \notin \delta_i \end{cases}, \tag{28}$$

where α are the nodes in the plane domain (x,y). Considering $\mathscr{T} = 2$, with $\chi_1 = \chi_s$ and $\chi_2 = \chi_p$, for soil and pipeline, respectively. The resulting weak form (Eq. (14)), reads now

$$-\int_{\Xi}\left[u^*\left(\rho_s\chi_s+\rho_p\chi_p\right)\omega^2 u + v^*\left(\rho_s\chi_s+\rho_p\chi_p\right)\omega^2 v + w^*\left(\rho_s\chi_s+\rho_p\chi_p\right)\omega^2 w\right] d\Xi =$$

$$-\int_{\Xi}\frac{\partial u^*}{\partial x}\left(\theta_s\chi_s+\theta_s\chi_s 2\iota\zeta_s+\theta_p\chi_p\right)\frac{\partial u}{\partial x}\,d\Xi$$

$$-\int_{\Xi}\frac{\partial v^*}{\partial y}\left(\lambda_s\chi_s+\lambda_s\chi_s 2i\zeta_s+\lambda_p\chi_p\right)\frac{\partial u}{\partial x}\,d\Xi$$

$$-\int_{\Xi}\frac{\partial w^*}{\partial z}\left(\lambda_s\chi_s+\lambda_s\chi_s 2i\zeta_s+\lambda_p\chi_p\right)\frac{\partial u}{\partial x}\,d\Xi - \ldots + \int_{\partial\Xi}\mathbf{u}^*\cdot(\sigma\mathbf{n})\,d(\partial\Xi), \tag{29}$$

where the boundary contribution (the last integral on $\partial\Xi$) involves expressions (19), (20) and (21), the last with unit components of the rock outcropping motion $\dot{\mathbf{y}}$ induced forces (first terms of the right had member of Eq. (21)), in order to obtain the parametric transfer function

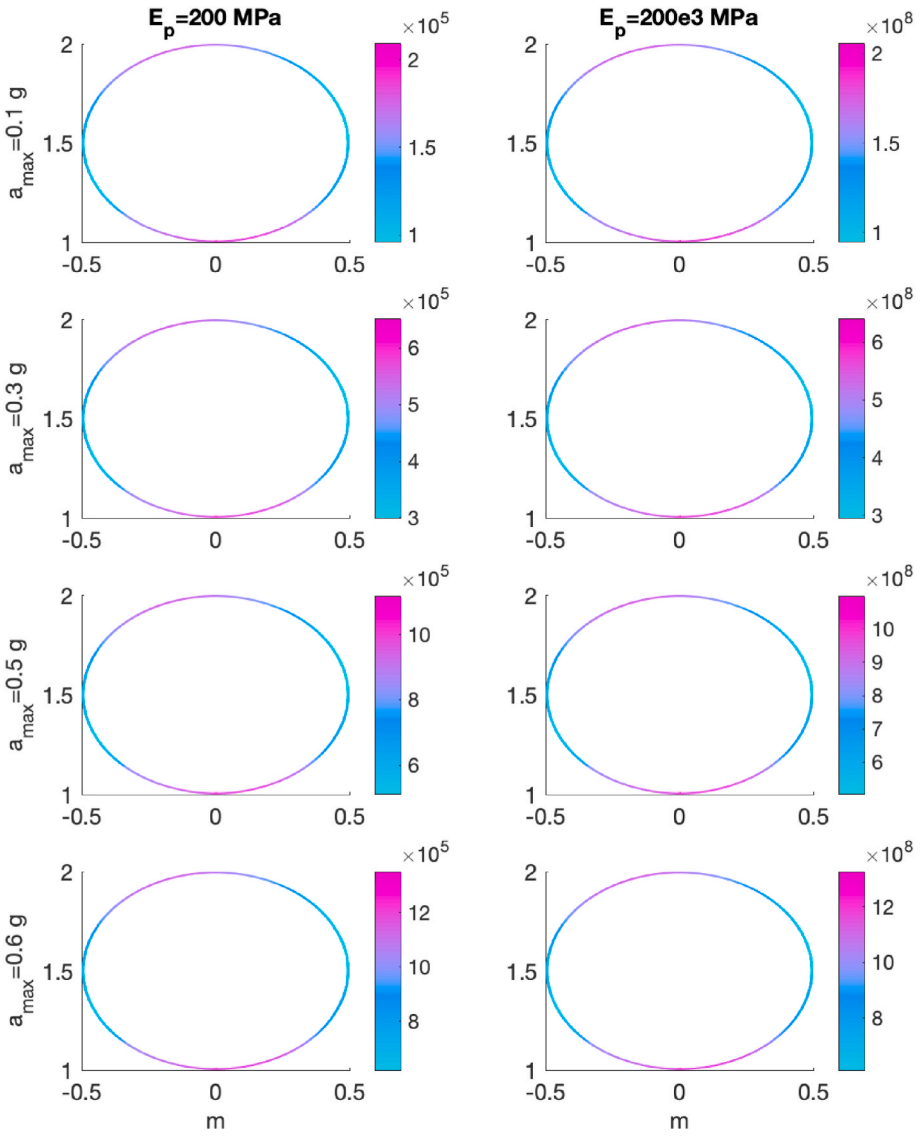

Fig. 5. Maximum principal stress in transverse cross section for different PGA values and pipeline elastic modulus.

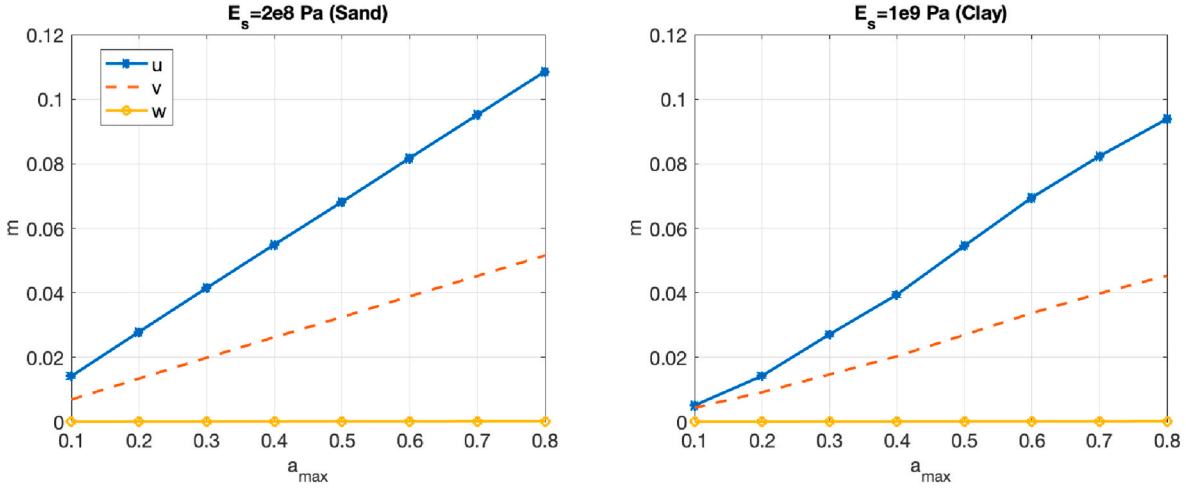

Fig. 6. Maximum displacement *u*, *v* and *w* for different soil materials.

able to be particularized in real-time, to obtain real-time responses.

Within the PGD-parametric setting, the extended domain reads $\Xi = \Omega_x \times \Omega_y \times \Omega_z \times \Omega_\omega \times \Omega_{E_s} \times \Omega_{\zeta_s} \times \Omega_{E_p} \times \Omega_{\rho_p}$ (with s and p the parameters related to the soil and pipeline) while its boundary $\partial\Xi = \partial(\Omega_x \times \Omega_y \times \Omega_z) \times \Omega_\omega \times \Omega_{E_s} \times \Omega_{\zeta_s} \times \Omega_{E_p} \times \Omega_{\rho_p}$.

The PGD solution in the separated form is

$$\mathbf{u}(x,y,z,\omega,E_s,\zeta_s,E_p,\rho_p) \approx \sum_{k=1}^{N} \mathbf{X}^k(x,y) \circ \mathbf{Z}^k(z) \circ \mathbf{W}^k(\omega) \circ \mathbf{E}_s^k(E_s) \circ \mathbf{C}_s^k(\zeta_s) \circ \mathbf{E}_p^k(E_p) \circ \mathbf{P}_p^k(\rho_p). \tag{30}$$

The PGD procedure for constructing the separated representation can be implemented as just described. In this case, the Proper Generalized Decomposition is able to circumvent the so-called curse of dimensionality in multi-dimensional spaces.

5. Real-time data update

As mentioned in Section 3.1, the nonlinear effects can be approximated by an equivalent linear analysis. The soil can be modeled as a function of the shear modulus reduction and an increase of damping ratio related with the effective of shear strain amplitude. Thus, the appropriate material curves given by Ref. [5] can be used iteratively to reach compatibility between the properties used in the analysis and the computed strain. Starting from initial small-strain values G_{max} and ζ (assuming linear regime) and then solving the dynamic problem, the effective shear strain, from the peak maximum, can be computed. Once the values of shear modulus G and damping ratio ζ have been updated, the process is repeated by particularizing the PGD parametric solution for the new couple of values, until converge has occurred, which usually occurs within 3 or 5 iterations.

The procedure is summarized below:

1. *Offline procedure:* PGD calculation of a monolayer parametric solution, $\mathbf{u}(x,y,z,\omega,E_s,\zeta_s,E_p,\rho_p)$.
2. *Online procedure:* Real-time dynamics for soil-pipeline interaction behavior:

1 Compute the Fourier transform of the input motion (in x, y, and z directions) given by (21),

$$\mathbf{F}(\omega) = \mathscr{F}(\mathbf{F}(\mathbf{t})). \tag{31}$$

2 Initialize from the small-strain elastic modulus E^0 and damping ratio ζ^0, and input the parameters that are assumed constants:

$$(E_s^0, \zeta_s^0, E_p, \rho_p). \tag{32}$$

3 Repeat the procedure until convergence:

- The complex displacement amplitude for each frequency of the input motion is computed from the parametric solution

$$\mathbf{u}(x,y,z,\omega,E_s^m,\zeta_s^m,E_p,\rho_p), \tag{33}$$

- where m is the nonlinear iteration. Applying the principle of superposition, the total response yields

$$\mathbf{u}^m(x,y,z,\omega) = \mathbf{F}(\omega) \circ \mathbf{u}(x,y,z,\omega,E_s^m,\zeta_s^m,E_p,\rho_p). \tag{34}$$

- Calculate the 6 strains component in the frequency domain from the displacement amplitudes at each element, from theses solutions the principal strains can be determined. Then, the corresponding effective shear strain is;

$$\gamma_{eff}(e) = \frac{2}{3}\frac{\max|\ddot{y}(t)|}{\mathrm{RMS}(\ddot{y})}\mathrm{RMS}(\gamma_{max}^*(e)). \tag{35}$$

- From $\gamma_{eff}(e)$ at each element, $e = 1, \ldots, N_e$, with N_e being the total number of elements, the maximum effective strain can be obtained, i.e., $\gamma_{eff} = max(\gamma_{eff}(e))$.
- Determine new strain values from the strain-dependent shear modulus and damping ratio curves [5] and then update the elastic modulus $E_s^{m+1} = 2G^{m+1}(1+\nu)$;
- The convergence criteria is given by $\mathscr{E}^m$:

$$\mathscr{E}^m = \left(\frac{|G^{m+1} - G^m|^2}{|G^1|^2} + \frac{|\zeta^{m+1} - \zeta^m|^2}{|\zeta^1|^2}\right). \tag{36}$$

4 Generate all outputs applying the inverse Fourier Transform.

6. Numerical example

To illustrate the potentialities of the algorithm here proposed, a parametric pipeline-soil model is considered. The approach described, was used to calculate the parametric solution of Eq. (30), given by $\mathbf{u}(xy,z,\omega,E_s,\zeta_s,E_p,\rho_p)$. The parametric domain is defined by $\Omega_{xy} = [0,6]^2$ mts, $\Omega_z = [0,20]$ mts, $\Omega_\omega = 2\pi(0,25)s^{-1}$, $\Omega_{E_s} = (100,1000)$ MPa, $\Omega_{\zeta_s} = (0.001,0.4)$, $\Omega_{E_p} = (200,2e5)$ MPa and $\Omega_{\rho_p} = (1000,7800)\ kg/m^3$. The different domains were discretized by considering respectively 1388, 500, 1024, 200, 200, 400 and 200 nodes. The Peak Ground Acceleration (PGA) is considered as a model parameter $a_{max} = [0.1,0.8]g$, which is used to scale the maximum value of the rock outcropping motion given in Fig. 2.

The solution is obtained assuming the horizontal acceleration time history in the outcropping is known, which correspond to x and z directions, vertical input motion (y direction) is assumed 2/3 the horizontal input motion. The pipeline elastic modulus and density were taken considering the values in Table 1. It is considered a pipe with 1 mt diameter and 1% thickness, buried at a depth of 1 mt (see Fig. 3) and soil density $\rho_s = 1900\ kg/m^3$.

6.1. Results

Fig. 4 illustrates the maximum stress (σ_x) values versus the pipeline elastic modulus and density, taking into account different initial values of soil elastic modulus and material curves, these results are taken from the top (x-y axes) and in the middle (z axe) of the pipeline. As observed an increase in the pipeline elastic modulus leads to increase the maximum stress values but for the pipeline density the changes are not significant. Similarly, the behavior varies depending on the soil stiffness and soil material, increasing soil stiffness generally results in more stress on the pipe.

The maximum principal stress in transverse cross section (in the middle of z axe) is shown in Fig. 5, in which an increase in the PGA but also the pipeline elastic modulus (from polyethylene to steel) leads to an increased tensile ring stresses.

Fig. 6 depicts the maximum displacement u, v and w versus different

PGA values, taking into account the constant values of $E_p = 2e5$ MPa and $\rho_s = 7800\,kg/m^3$, in this case the displacement values increase regarding the soil stiffness as well as the maximum acceleration.

The main advantage of the PGD technique is the off-line approach that allows obtaining parametric solutions for the pipeline-soil model, considering all model parameters. As soon as these solutions are available, the results can be obtained by particularizing the parametric solutions in an instantaneous manner (real time). The resulting problem is in a 8-dimensional space and the obtained parametric solution is able to described 2.2e18 possible scenarios. The memory required to store this solution is negligible with what would be required for an equivalent 8 dimensional grid.

8. Conclusions

This paper proposes a new dynamic analysis for buried pipeline considering the nonlinear soil interaction. Model parameters have been considered as extra-coordinates for constructing very rich parametric solutions which can be used in real time. The numerical algorithm capabilities for computing a fine enough 3D solution is based on the use of in-plane-out-of-plane separated representations within the PGD technique, that permitted overcome the difficulties related to the large numbers of degrees of freedom of fully 3D mesh, reducing the problem to a 2D cost. This method can be used to identify suitable material combinations based on their potential stress reduction and displacements.

Funding

This study is funded by grants from the INTEC research fund under the project ING-330533-2018-P-1.

Declaration of competing interest

The authors declare that they have no known competing financial interests or personal relationships that could have appeared to influence the work reported in this paper.

Acknowledgements

The authors are grateful for the support and collaboration of the National Fund for Innovation and Scientific and Technological Development (FONDOCYT) in Dominican Republic, through project No. 2016-2017-071.

References

[1] Ansal A, Kurtuluş A, Tönük G. Damage to water and sewage pipelines in Adapazari during 1999 Kocaeli, Turkey earthquake. 2008.
[2] Applied Technology Council. Seismic vulnerability and impact of disruption of lifelines in the conterminous United States. 1991. ATC-25.
[3] Bian X, Chen Y, Ye X. Environmental vibrations and transportation geodynamics. Springer; 2007.
[4] Bognet B, Leygue A, Chinesta F, Poitou A, Bordeu F. Advanced simulation of models defined in plate geometries: 3D solutions with 2D computational complexity. Comput Methods Appl Mech Eng 2012;201:1–12.
[5] Bradet JP, Ichii K, Lin CH. EERA: A computer program for equivalent-linear earthquake site response analyses of layered soil deposits. University of Southern California, Department of Civil Engineering; 2000.
[6] Bognet B, Leygue A, Chinesta F. Separated representations of 3D elastic solutions in shell geometries. Adv Model Simul Eng Sci 2014;1:4.
[7] Bordeu F, Ghnatios Ch, Boulze D, Carles B, Sireude D, Leygue A, Chinesta F. Parametric 3D elastic solutions of beams involved in frame structures. Adv Aircr Spacecr Sci 2015;2(3):233–48.
[8] Chen, W. W., Shih, B. J., Chen, Y. C., Hung, J. H. and Hwang, H. H. Seismic response of natural gas and water pipelines in the Ji-Ji earthquake. Soil Dynam Earthq Eng; 22: 1209-1214.
[9] Chinesta F, Ammar A, Cueto E. Recent advances and new challenges in the use of the Proper Generalized Decomposition for solving multidimensional models. Arch Comput Methods Eng 2010;17/4:327–50.
[10] Chinesta F, Leygue A, Bordeu F, Aguado JV, Cueto E, Gonzalez D, Alfaro I. Parametric PGD based computational vademecum for efficient design, optimization and control. Arch Comput Methods Eng 2013;20/1:31–59.
[11] Chinesta F, Keunings R, Said P. The Proper Generalized Decomposition for advanced numerical simulations. A primer, Springerbriefs. Springer; 2014.
[12] Germoso C, Aguado JV, Fraile A, Alarcon E, Chinesta F. Efficient PGD-based dynamic calculation of non-linear soil behavior. Compt Rendus Mec 2016;344(1):24–41.
[13] Fares R, Deschamps A. Soil-structure interaction analysis using a 1DT-3C wave propagation model. Soil Dynam Earthq Eng 2019;120:200–13.
[14] Idriss I, et al. Quad-4: a computer program for evaluating the seismic response of soil structures by variable damping finete element procedures. University of California; 1973.
[15] Isenberg J, Richardson E, Kameda H, Sugito M. Pipeline response to loma Prieta earthquake. J Struct Eng 1991;117(7):2135–48.
[16] Joyner WB, Chen A. Calculation of nonlinear ground response in earthquakes. Bull Seismol Soc Am 1975;65(5):1315–36.
[17] Kagawa T, et al. TLUSH: a computer program for the three-dimensional analysis of earth dams. Berkeley: University of California; 1981. Report No. UCB/EERC-81-14.
[18] Kramer SL. Geotechnical earthquake engineering. Pearson Education India; 1996.
[19] Leygue A, Chinesta F, Beringhier M, Nguyen NL, Pasavento F, Schrefler B. Towards a framework for non-linear thermal models in shell domains. Int J Numer Methods Heat Fluid Flow 2013;23(1):55–73.
[20] Lysmer J, Kuhlemeyer AM. Finite dynamics model for infinite media. J Eng Mech 1969;95:859–77.
[21] Lysmer J, et al. FLUSH-A computer program for approximate 3-D analysis of soil-structure interaction problems. California Univ.; 1975.
[22] Miura K, Kobayashi S, Yoshida N. Equivalent linear analysis considering large strains and frequency dependent characteristics. In: Proceeings 12-th world conference on earthquake engineering; 2000. p. 1832. Auckland, New Zealand, Paper.
[23] Moravec F, Letzelter N. On the modeling of the linear viscoelastic behaviour of biological materials using Comsol Multiphysics. Applied and Computational Mechanics; 2007.
[24] Pruliere E, Chinesta F, Ammar A. On the deterministic solution of multidimensional parametric models using the proper generalized decomposition. Math Comput Simulat 2010;81(4):791–810.
[25] Santisi d'Avila MP, Lenti L, Semblat JF. Modeling strong seismic ground motion: 3D loading path vs wavefield polarization. Geophys J Int 2012;190:1607–24.
[26] Schnabel, P.B., Lysmer, J. and Seed, H.B. SHAKE-91: Equivalent Linear Seismic Response Analysis of Horizontally Layered Soil Deposits. The Earthquake Engineering Online Archive NISEE e-Library, http://nisee.berkeley.edu/elibrary/Software/SHAKE91ZIP.
[27] Shih JY, Thompson DJ, Zervos A. The effect of boundary conditions, model size and damping models in the finite element modelling of a moving load on a track/ground system. Soil Dynam Earthq Eng 2016;89:12–27.
[28] Shinozuka M, Ballantyne D, Borcherd R, Buckle I, O'Rourke T, Schiff A. The Hanshin-Awaji earthquake of January 17, 1995. Performance of lifeline. Tech Rep 1995:225. NCEER, Buffalo, NY, USA.
[29] Trifunac MD, Todorovska MI. Northrige, California, earthquake of 1994: density of Pipe breakes and surface strains. Soil Dynam Earthq Eng 1997;16:193–207.
[30] Yoshida, N., Kobayashi, S. , Suetomi, I., Miura, K.Equivalent linear method considering frequency dependent characteristics of stiffness and damping. Soil Dynam Earthq Eng, 22(3), 205-222.